GEOSPATIAL MODELING OF SOIL EROSION DYNAMICS IN THE KALASH RIVER WATERSHED OF DISTRICT CHITRAL, PAKISTAN

MUHAMMAD SHABIR¹, MUHAMMAD JAMAL NASIR², SAMI-UL-HAQ³, MUHAMMAD IBRAHIM^{4*}

¹²³Department of Geography and Geomatics, University of Peshawar, Peshawar, Pakistan

⁴Department of Urban and Regional Planning, University of Peshawar, Peshawar, Pakistan

Corresponding author e-mail: plnr.ibrahim1@gmail.com

ABSTRACT

Land and water are vital natural resources, yet poor management often leads to severe degradation, threatening both ecosystems and food security. In this study, we estimated annual soil loss in the Kalash River Watershed (KRW), Lower Chitral District, Pakistan, using a GIS-based Sediment Production Rate (SPR) approach. The SPR model relies on three key morphometric parameters: form factor (Rf), circulatory ratio (Rc), and compactness coefficient (Cc). We derived the drainage network, watershed boundary, and all morphometric indices from the ALOS PALSAR Digital Elevation Model (12.5 m resolution). Results show the basin has a semi-circular to slightly elongated shape (Rf = 0.65, Rc = 0.52, Cc = 1.38), which directly influences runoff concentration and sediment transport patterns. The watershed exhibits low stream frequency (0.14 streams/km²) and drainage density (0.38 km/km²), pointing to a somewhat restricted drainage network and predominantly localised erosion. Bifurcation ratios ranging from 3.65 to 8.73 further suggest structural controls on drainage development that affect sediment distribution. The calculated Sediment Production Rate of 0.43 hectare-metres per 100 km² per year indicates moderate erosion risk, highlighting the need for targeted conservation interventions. We recommend integrated measures such as terracing, construction of check dams, and afforestation to reduce soil loss effectively. Overall, the findings underline the importance of sustained watershed management to control sedimentation, stabilise water resources, and boost agricultural productivity. In the Kalash valleys, future work combining hydrological modelling and advanced remote sensing could refine erosion forecasts and support adaptive planning. This study provides decision-makers with critical, evidence-based insights for implementing effective soil conservation strategies and ensuring long-term environmental sustainability in the region.

KEYWORDS: Stream Power Index, Sediment Transport Index, Soil Erosion, Sediment Production Rate, Morphometry, GIS/RS, Kalash River Watershed

1. INTRODUCTION

In mountainous regions, soil erosion is a primary driver of land degradation, which directly impacts agricultural productivity, stability of slopes, reservoir sedimentation and downstream flood risk (Kumar et al.,

2023). The Hindu Kush and Karakoram regions are a case of a high mountain environment where processes like accelerated snow and glacier retreat, more intense precipitation events, and expanding bare and degraded surfaces intensify surface runoff and sediment mobilization, increasing the frequency and magnitude of erosion events (Mehwish et al., 2024; Ashraf & Ahmad, 2024). These dynamics make watershed management more difficult under climate change and endanger community livelihoods and infrastructure in headwater catchments.

The Kalash River Watershed is a vital natural resource for biodiversity, carbon sequestration, water management, and agricultural production. A vital natural resource, good soil is the foundation of terrestrial ecosystems and supports over 95% of the world's food production. It also acts as a significant carbon sink, storing more carbon than the atmosphere and plants put together (Rojas et al., 2016). Additionally, by enhancing infiltration and reducing runoff, soil helps filter water and mitigate floods (Tedoldi et al., 2016).

Despite its significance, important ecosystem processes are seriously threatened by soil degradation, especially erosion. Rich topsoil is lost at rates far higher than natural replacement due to soil erosion brought on by deforestation, subpar farming practices, and climate change (Musa et al., 2024). According to Borrelli et al. (2017), excessive cultivation and monocropping further undermine soil structure, and removing vegetation exposes soil to wind and water erosion. Wide-ranging effects of unchecked decreased erosion include agricultural vields, increased sedimentation, and annual economic losses estimated at \$400 billion (Handelsman, 2021). Additionally, pollutants that deteriorate water quality and impact aquatic ecosystems are often present in eroding sediments (Rashmi et al., 2022).

Strategies for mitigation are essential to preventing long-term harm to soil resources because soil formation is slow; it can take up to 1,000 years to create a few millimetres. It has been demonstrated that conservation agriculture, which includes cover crops and no-till farming, improves soil health while reducing erosion (Carceles et al., 2022). Although policy intervention is necessary to promote sustainable land management, terracing and afforestation also aid in soil stabilization (Sanz et al., 2017). Persistent soil deterioration would endanger global food security, exacerbate climate change, and disrupt water cycles if quick action is not taken. To maintain long-term environmental sustainability and human

well-being, soil conservation must be given top priority through scientific, agricultural, and regulatory methods.

Natural elements like wind and water, as well as human activities like deforestation and unsustainable farming practices, can cause soil erosion by shifting the topsoil layer (Pimentel & Burgess, 2013). Aquatic ecosystems may be impacted by this process's effects on soil fertility, agricultural output, and sedimentation in water bodies (Siebielec et al., 2016). The Food and Agriculture Organization (FAO, 2015) estimates that around 0.075 trillion tons of soil are lost each year, with agricultural land being the most impacted.

To evaluate spatial patterns of soil loss over diverse terrain, geospatial modeling has become common practice. By incorporating rainfall erosivity, soil erodibility, slope length and steepness, cover management, and conservation practice parameters, the Revised Universal Soil Loss Equation (RUSLE) offers a useful, spatially explicit estimate of yearly soil loss when combined with remote sensing and GIS (Naqvi et al., 2024). While admitting its limits in event-based prediction and sediment routing, RUSLE-GIS studies in semi-arid and mountainous locations have shown its value in detecting erosion hotspots and prioritizing conservation (Zineddine, 2025).

RUSLE-based mapping is strengthened by recent methodological developments that improve computing platforms and data inputs. Model repeatability and spatial detail have been enhanced using high-resolution DEMs, time-series land use/land cover data from Sentinel and Landsat archives, cloud platforms like Google Earth Engine for bulk processing, and enhanced rainfall erosivity datasets (Nigussie et al., 2025). Scalable methods for creating policy-relevant maps for vast and distant watersheds are provided by hybrid systems that combine RUSLE with multi-criteria decision analysis or cloud-based geospatial operations (Boota et al., 2024).

Gilani et al. (2022) determined the rate of soil loss in several Pakistani administrative units between 2005 and 2015 using the Revised Universal Soil Loss Equation (RUSLE). The study highlights the region most vulnerable to land degradation by demonstrating significant variations in soil erosion. Khyber Pakhtunkhwa (KP) had a significant rise from 8.73 ± 25.55 to 12.84 ± 39.88 tons/ha/year, attributed to agricultural growth, landslides, and monsoon rainfall in steep areas. In Gilgit-Baltistan (GB), glacial melt and unregulated development in sensitive alpine habitats led to a surge from 7.54 ± 20.25 to 9.06 ± 29.69 tons/ha/year. Pakistan's average soil erosion rate rose from 1.79 ± 11.52 to 2.47 ± 18.14 tons/ha/year, showing

worsening land degradation. The steepest increases occurred in hilly and rain-fed regions (AJK, KP, Gilgit Baltistan), stressing the importance of terracing, afforestation, and sustainable farming to reduce erosion.

Several quantitative and process-based models are used to calculate soil loss and sediment output. The Universal Soil Loss Equation (USLE) and its updated version, known as Revised Universal Soil Loss Equation (RUSLE), are commonly used to forecast yearly soil loss, and newer research has combined GIS and RS to improve accuracy. The Soil and Water Assessment Tool (SWAT) are a semi-distributed model that simulates sediment yield using climate, soil, and land management variables. Global assessments such as GLASOD (Global Assessment of Soil degradation) gave early qualitative evaluations of human-induced degradation of soil, but more modern models like GloSEM (Global Soil Erosion Modelling) give highresolution, RUSLE-based quantitative estimates. In contrast to these hillslope-focused models, SedNet (Sediment Network Model) provides a comprehensive sediment budget by assessing erosion, transport, and deposition at the catchment scale. These models are critical for understanding erosion dynamics, developing conservation policies, and minimizing environmental consequences.

Another method, the Sediment Production Rate (SPR), estimates sediment production from individual erosion sources using sediment delivery ratios (SDRs), with geospatial technologies increasing estimation using high-resolution DEMs and satellite-derived land-use data. This research aims to assess the annual soil loss from the KRW using a GIS-based Sediment Production Rate (SPR), Sediment Power Index (SPI), and Stream Transport Index (STI) approaches.

The use of machine learning and hybrid approaches to predict sediment yield and erosion susceptibility has grown considerably in recent years (Hitouri et al., 2022). Where field measurements are available, researchers have successfully applied tree-based algorithms and other supervised methods to map erosion risk (Eloudi et al., 2023). These techniques are particularly good at capturing complex, non-linear relationships between topography, climate, soil properties, and land-cover, something traditional empirical models often struggle with. That said, achieving reliable transferability in data-scarce mountain catchments still requires rigorous cross-validation and independent testing against actual soil and sediment loss measurements (Hasnaoui et al., 2025).

Recent work on land-use changes and snow-cover dynamics in the Chitral region shows a clear trend: declining snow and natural vegetation cover coupled with expanding built-up areas and bare soil, all of which leave slopes more prone to instability and surface erosion (Aslam et al., 2021). Local studies that applied RUSLE in a GIS environment have already documented rising soil-loss rates in parts of the Chitral basin, underlining the need for high-resolution, catchment-scale assessments that combine remote sensing, ground-truthing, and climate-change scenarios (Maqsoom et al., 2020; Kousar & Shirazi, 2023). The present study builds directly on these efforts by delivering a geospatial RUSLE application specifically for the Kalash River watershed, using the latest high-resolution datasets and producing detailed, spatially explicit erosion-risk maps to guide targeted conservation and management actions.

2. STUDY AREA

The KRW is situated approximately 30 km downstream of Chitral town. The watershed is located between 35°-35' to 35°-50' North Latitude and 71°-30' to 71°-46' East longitude. The height of the watershed varies between 1393 m to 5351 m above sea level. The valley is characterized by steep slopes, narrow gorges, and rugged terrain. The KRW is surrounded by the Hindukush Mountain range. It comprised two valleys. The largest and most popular valley is Bumburet, reached by a road from Ayun on the main Chitral-Drosh road. Rumbur is a side valley north of Bumburet. To the North of the watershed lies Chitral Gol National Park; to the east, it shares its border with Afghanistan; to the west is the river Chitral, and to the southeast is the valley of Birir. The valley is home to the Kalash people, an indigenous group known for their distinct cultural and religious traditions. The geographic isolation of the region has contributed to the preservation of its unique way of life. The Kalash Valley remains a significant area of cultural and anthropological interest due to its remote location and the traditional practices of its inhabitants. The Kalash people, an indigenous community in northern Pakistan, have preserved a rich cultural heritage that extends back over 2000 years. Their traditions reflect a deep connection to nature, ancestral customs, and a unique polytheistic (worshipping or believing in more than one God) belief system distinct from the surrounding regions.

Figure 1 shows the data type and its attributes, which will be collected from various online sources. The study is entirely dependent on secondary data. Digital Elevation model (DEM) was the main source of data, which

was used to derive the drainage network and delineation of the watershed boundary.

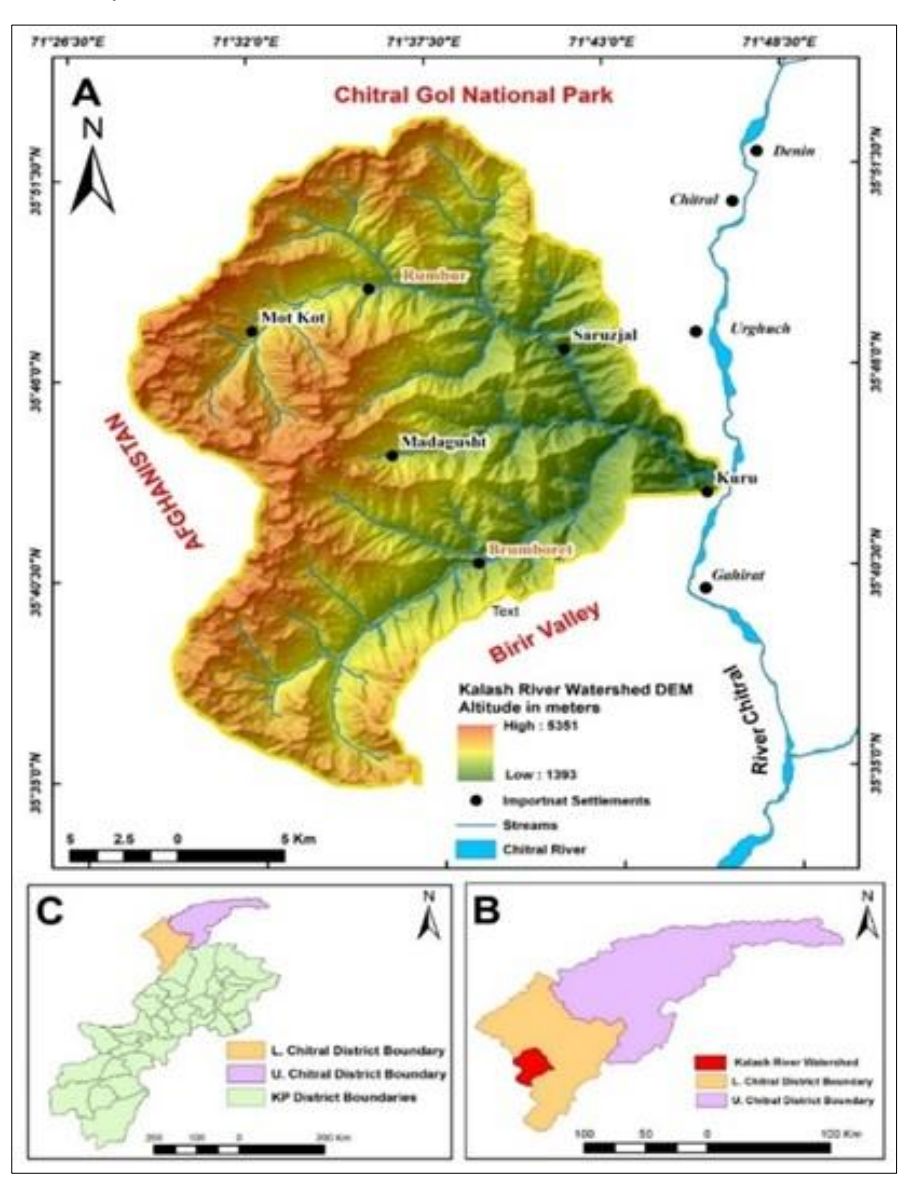


Figure 1. (A) Location of the Kalash River Watershed (KRW); (B) Lower and Upper Chitral Districts showing the study area; (C) District map of Khyber Pakhtunkhwa highlighting Chitral Lower and Upper

3. MATERIAL AND METHODS

3.1 Data Collection

Table 1 data type, data source, its attributes, and its usage for the derivation of various morphometric parameters. Table 2 shows the

computed morphometric parameters, their formula / empirical equation used to calculate these parameters for the KRW.

Table 1: Depicts the Derived DEM, its attributes, and the source

S.	Data	Source	Attributes	Usage
No	Type			
1	DEM	The ALOS PALSAR	12.5-	Drainage Network, Watershed
		Digital Elevation	meter	Boundary, Watershed Perimeter,
		Model (DEM) 12.5m	Resolution	Stream order, Stream length,
		was acquired from the		Stream numbers, Bifurcation
		Alaska Satellite		Ratio, Stream Density, Stream
		Facility.		Frequency, Form Factor,
		https://asf.alaska.edu/		Circularity Ratio, Compactness
				Coefficient

Source: https://asf.alaska.edu/

Table 2: Depicts the selected morphometric parameters and their formula

S.	Morphometric	Formula/Definition	References
No	Parameters	· ·	
1	Basin area km² (A)	Area of the watershed (km²)	Horton (1945)
2	Basin perimeter km (P)	Perimeter of the watershed (km)	Horton (1945)
3	Basin Length Km Length of the basin (km) (L²)		Horton (1945)
4	Drainage Density Stream Drainage Density (Fs = Lu / A)		Strahler (1964)
4	Form factor (ratio) (Rf)	Rf = A / L ² where A is the Drainage basin area, L ² Length of the Drainage basin	Strahler (1964);
5	Circularity Ratio (Rc)	Circulatory Ratio (Rc) = $4\pi A / P^2$ Where A is the area of the sub - basin P is the perimeter of the sub - basin and π is the mathematical constant, (approx = 3.14159)	Strahler (1964); Faniran (1968)
6	Compactness coefficient (Cc)	(Cc) = P / $[2(\pi A)^0.5]$ Where P is the Watershed Perimeter and A is the area of the watershed	Strahler (1964); Faniran (1968)

Source: Analysis of DEM in the Arc Hydro tool in ArcMap 10.8

3.2 Data Analysis

The following steps were involved in the derivation of the drainage network and the delineation of the watershed boundary from the DEM in ArcMap 10.8, using the Arc Hydro Tools

3.2.2 Data acquisition

The main dataset used in this study is the 12.5 m resolution ALOS PALSAR Digital Elevation Model (DEM), which we downloaded from the Alaska Satellite Facility (ASF). We started by preprocessing the DEM. The key step was filling sinks to get rid of any artificial depressions that can mess up hydrological modelling. Once that was done, we calculated the flow direction to show how water would move across the surface. Next, we derived flow accumulation, which helped highlight where water concentrates and forms channels. With the flow accumulation grid ready, we extracted the stream network by choosing a suitable threshold value that separates real streams from minor overland flow. The streams were then ordered (Strahler method) and segmented into individual links to build a proper hydrological structure. After that, we generated a catchment grid that defines the contributing area for every stream segment and cleaned up the drainage lines to ensure a continuous, logical network with no breaks. Finally, using all these corrected hydrological layers, we delineated the exact boundary of the Kalash River Watershed (KRW).

3.3. Derivation of Secondary Parameters

The secondary parameters, including bifurcation ratio, drainage density, and drainage frequency, were computed using the formulas stated in Table 2. The three important parameters necessary for sediment production rate were: Circulatory Ratio, Form Factor, and Compactness coefficient. Figure 2 illustrates the research methodology flowchart. The workflow involved DEM preprocessing, watershed delineation, morphometric analysis, SPI/STI calculation, and spatial classification of erosion risk.

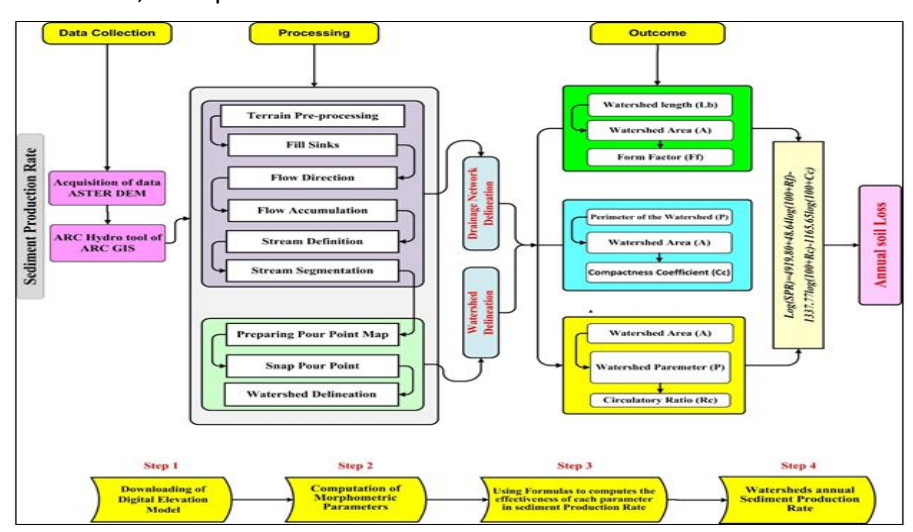


Figure 2: Illustrating Methodology Flowchart

4. RESULTS AND DISCUSSION

4.1. Kalash River Watershed Characteristics

4.1.1 Stream Order

Stream Order is a classification system used in hydrology and geomorphology to quantify the hierarchical position of a stream within a river network. It helps in understanding the structure and complexity of drainage systems. The most used methods for stream ordering are those devised by Strahler (1964) and Horton (1945) stream order systems. However, for the present study, the most widely used Strahler Stream Order system is used. According to Strahler stream order, headwater streams (the smallest, unbranched tributaries) are assigned order 1. When two first-order streams combine, it becomes a second-order stream, and when two second-order streams combine, it becomes a third-order stream, and so on. Table 3 depicts the stream ordering system of the KRW. The table provides a summary of the stream network hierarchy in the KRW using the Strahler stream ordering system. The analysis reveals that the watershed has a 4th-order stream, and the Kalash River is a 4thorder stream. The total stream lengths (in kilometres) for each stream order in the KRW reveal key insights into the basin's hydrological structure. The watershed has 93.92 km of first-order (I) streams, forming the extensive headwater network. As stream order increases, the cumulative length decreases, with 47.46 km of second order (II) streams, formed by the convergence of first-order channels. The third order (III) streams have a length of 34.95 km, indicating further integration of flow into fewer but larger channels. The fourth order (IV) streams have a length of 22.05 km. The total length of all the streams in the KRW is 198.38 km. This pattern generally follows Horton's laws, which suggests that in a well-developed drainage basin, the mean stream lengths in successive orders tend to follow a direct relationship, i.e., the length increases as the stream order increases. Figure. 3 and 4 illustrate the stream ordering system of the KRW. According to the data, the watershed contains 64 first-order (I) streams. These first-order streams converge to form 13 second order (II) streams, indicating that two or more first-order streams have merged. Further downstream, the second-order streams combine to create 4 thirdorder (III) streams, and finally, these third-order streams join to form a single fourth-order (IV) stream, representing the highest-order channel in the watershed. This distribution follows Horton's laws of stream numbers, which suggests an inverse relationship between the number of streams in successive stream orders, i.e., the number of streams decreases as stream order increases. The higher number of first-order streams highlights the watershed's highly branched, dendritic drainage pattern, typical of natural river systems. The presence of only one fourth-order stream suggests a relatively small to medium-sized basin, where higher-order channels integrate flow from numerous smaller tributaries. The Kalash River combines with the Chitral River near Ayun, a small village located some 25 km downstream of Chitral Town.

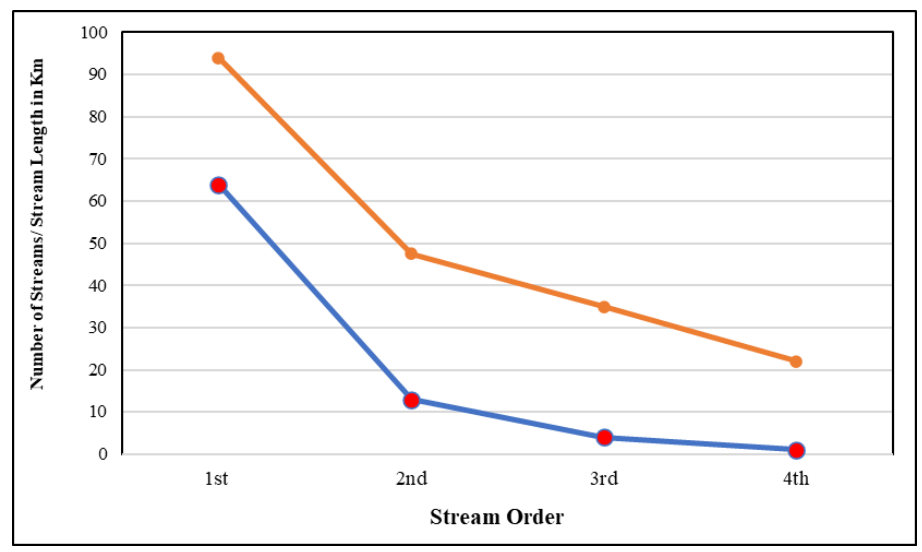


Figure 3. illustrates the stream ordering system of the KRW

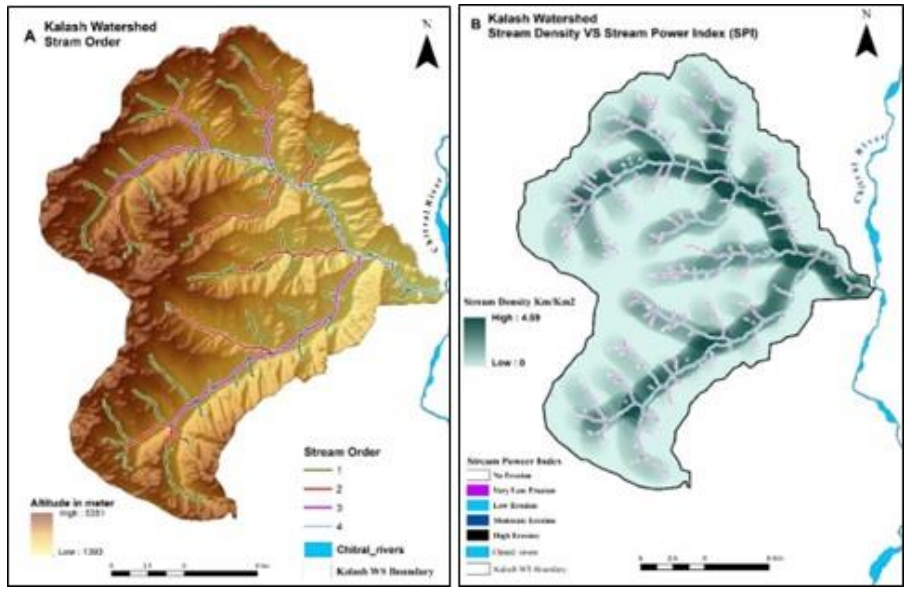


Figure 4. illustrates the stream ordering system, stream density, and stream power Index of the KRW

4.1.2 Bifurcation Ratio (Rb)

Table 3 also presents the R_b for each stream order in the KRW, revealing key structural properties of its drainage network. The R_b is a fundamental concept in fluvial geomorphology, defined as the ratio of the number of streams of a given order (N_u) to the number of streams of the next higher order (N_{u+1}) . Mathematically, it is expressed as (Horton, 1945):

$$Rb = \frac{Nu}{Nu+1}$$
.....Equation. 1

The analysis reveals that the Rb ratio between I order and II order streams is 1.46, slightly low, suggesting moderate branching. The Rb ratio between the 2nd order and 3rd order is 3.65 (within the typical Horton range of 3–5). The Rb ratio between the 3rd order and 4th order is 8.73 (unusually high, indicating a sudden drop in stream count. The mean R_b of the KRW is 4.5, is aligns with natural dendritic basins. A low Rb (close to 2) implies a welldrained, uniform basin (e.g., homogeneous geology). A high Rb (≥5) suggests structural control (e.g., tectonic faults, resistant rock) limiting tributary development (Akhtar et al., 2024). The unusually high R_b ratio (8.73) between 3rd and 4th order streams indicates a rapid merging of streams into a few major channels, possibly due to a mountainous valley restricting tributary formation. Hydrologically high bifurcation ratios correlate with flashier flood responses (rapid flow concentration). Watersheds with irregular Rb may exhibit uneven sediment distribution and erosion patterns.

Table 3: Kalash River Watershed, Drainage System

S.	Morphometric	Mean		Stream	Orders		Total
No	Parameters		ı	II	III	IV	
1	Stream Order		ı	II	Ш	IV	IV
2	Number of Stream (Nu)		64	13	4	1	72
3	Stream Length (Lu)		93.92	47.46	34.95	22.05	198.38
4	Mean Stream Length ()	2.75	1.46	3.65	8.73	22.05	
5	Bifurcation Ratio (R _b)	4.05	-	4.9	3.25	4	
	Watershed Area		511.72 km	1 ²			

Source: DEM analysis in the Arc Hydro tool of ArcMap 10.8.2

4.1.3 Watershed Area

The computed area of the KRW is 511.72 Km². Watershed area plays a crucial role in determining soil erosion, flash floods, and the region's hydrological dynamics. The size of the watershed directly influences the

quantity and speed of surface runoff, which can worsen soil erosion, especially in areas with steep slopes, deforestation, or poor land management. Heavy rainfall events can cause significant sediment movement, which can lower soil fertility and exacerbate sedimentation in rivers and lakes downstream. Additionally, due to the large watershed area, heavy or prolonged rainfall can accumulate large amounts of water, increasing the risk of flash floods, especially if the area has congested natural drainage systems or sparse vegetation cover that cannot absorb excess moisture (Nasir et al., 2025). Hydrologically speaking, the watershed is an important catchment that regulates streamflow, groundwater recharge, and seasonal water availability (Waikar & Nilawar 2014).

4.1.4 Watershed Perimeter

The KRW's 110.67 km circumference is an important morphometric component that influences the basin's shape, drainage characteristics, and hydrological activity. Morphometric analysis uses the perimeter and area to calculate the form factor (Ff), elongation ratio (Re), and compactness coefficient (Cc), which assess the shape and runoff capacity of a watershed and eventually estimate the sediment production in a watershed. As in the case of Kalash, which has an area of 511.72 km² and a longer perimeter than area, this suggests an elongated or irregular basin structure, which frequently has lower peak flows and longer lag periods than circular basins. Although this elongation lowers the risk of flooding, different flow velocities may cause soil erosion in some parts of the basin. The perimeter also influences stream frequency (Fs) and drainage density (Dd), which show how well the watershed conveys water. Higher perimeter-to-area ratios may indicate more intricate stream networks and possible patterns of sediment distribution, which might impact land degradation and sedimentation (Shekar & Mathew 2024). Therefore, perimeter analysis in morphometric studies aids in the comprehension of erosion patterns, flood susceptibility, and sustainable watershed management techniques.

4.1.5 The Circulatory Ratio (Rc)

One MP used to evaluate a watershed's form is the Rc. It sheds light on its potential for soil erosion, hydrological behavior, and vulnerability to flash floods. The ratio of the watershed area to the area of a circle with the same perimeter as the watershed is known as Rc (Miller, 1953). A watershed that is more circular is indicated by a value around 1, but an extended form is suggested by lower values. Circular watersheds are more susceptible to flash floods due to the rapid concentration of runoff due to their shorter flow paths and higher peak discharge rates (Horton, 1945). Conversely, longer watersheds have slower reaction times, which reduce

peak flows but may exacerbate soil erosion due to the longer water movement across slopes (Strahler, 1964). It evaluates the drainage effectiveness and runoff concentration of a watershed.

The study indicates that concentrated overland flow is more likely to cause considerable soil erosion in watersheds with high Rc values, whereas more dispersed but persistent erosion may occur in watersheds with low Rc values (Jothimani et al., 2020). Additionally, the Rc influences the dynamics of sediment transport; at times of high rainfall, circular basins often produce more material (Farhan & Anaba, 2016). Therefore, understanding Rc is crucial for managing watersheds because it enables more effective mitigation strategies by forecasting erosion patterns, hydrological responses, and flash flood hazards.

The Rc, a morphometric ratio, measures how closely the form of a watershed matches a complete circle. It is expressed empirically in Equation 2:

$$R_c = \frac{4\pi A}{P^2} \dots \dots Equation. 2$$

Where A is the Area of the watershed in Km²

and P is the watershed perimeter in Km

 π is the mathamatical constant (approximatly 3.14159)

 $Kalash\ watershed\ area=511.72\ km^2$

 $Watershed\ Perimeter = 110.67\ km$

$$Rc = \frac{4 \times 3.14159 \times 511.72}{(110.67)^2}$$
$$Rc = \frac{6430.45}{12247.84}$$
$$Rc = 0.52$$

The watershed is semicircular or elongated rather than circular when the Rc value is 0.52; a more circular shape is suggested with a Rc value closer to 1 (Miller, 1953). The dynamics of soil erosion throughout the watershed are significantly impacted by this elongation.

4.1.6 Form Factor

An MP called the Form Factor (Ff) compares a watershed's area to the square of its maximum length to characterize its shape (Horton, 1945). The form factor is calculated by using the following equation 3:

$$Ff = \frac{A}{L^2} \dots \dots Equation.$$

Where A is the Area of the watershed in Km^2 , and L is the watershed Length in Km

Kalash watershed area $(A) = 511.72 \text{ km}^2$, Watershed Length (L) = 27.85 km

$$Ff = \frac{511.72}{(27.85)^2}$$
$$Ff = \frac{511.72}{775.62}$$

Ff = 0.65, Ff's value falls between ~0.79 (completely round) and 0 (very elongated). Runoff behaviour, peak discharge, and soil erosion processes are all significantly impacted by the watershed's form, as shown by Ff.

Elongated watersheds are indicated by a lower Ff value of less than 0.3, which suggests longer flow routes and delayed peak runoff (Strahler, 1964). However, water flows along slopes for longer periods of time, which increases rill and sheet erosion (Morgan et al., 1998). Aggradation, or sediment building, occurs in riverbeds because of the silt being carried over longer distances (Singh & Singh, 2018). Soil loss is mild but persistent due to erosion, which is less concentrated but more pervasive across slopes (Rai et al., 2017).

A circular or semi-circular watershed, which permits faster runoff convergence and larger peak flows, is indicated by a higher form factor value (Horton, 1945). This results in significant gully erosion at the outlet due to the concentrated flow (Wischmeier & Smith, 1978). Silt is quickly transported downstream during storms, increasing the amount of sediment produced. The rapid response makes bank erosion and scouring worse, especially in downstream areas. Soil erosion dynamics and hydrological behavior are significantly impacted by the KRW's semi-circular to substantially circular watershed form, as shown by its Form Factor (Ff) of 0.65. Compared to elongated basins (low Ff), this morphology results in bigger peak discharges, faster runoff concentration, and more intense erosion near the outflow. The following are the principal consequences:

Because of the near-circular form, rainfall runoff reaches the outlet more quickly, resulting in higher peak flows (Horton, 1945). The rapid water convergence increases channel shear stress, which results in channel

widening and bank erosion, and thus increases the risk of flash floods, especially during powerful storms (Grecu et al., 2017). This converging flow pattern at the watershed outlet causes concentrated erosion, which leads to gully development (Morgan et al., 1998). Because degraded soil is swiftly carried downstream in elongated basins, sediment production is larger than in rounded basins. Due to shorter flow routes, a high form factor (Ff > 0.5) increases surface runoff volume by reducing the amount of time that precipitation may penetrate the soil (Wischmeier & Smith, 1978). Before water accumulates in channels, this causes increased soil erosion in highland locations. Sediment deposition is negligible, and most of the eroded material is moved downstream, resulting in increased sediment transport, because of the high hydraulic gradient and fast flow (Merritt et al., 2003).

4.1.7 Compactness Coefficient

A morphometric statistic called the Compactness Coefficient (Cc), often referred to as the Gravelius Index, is used to evaluate a watershed's form by comparing its perimeter to that of a circular watershed with the same area. Higher values (>1) suggest more extended or irregular geometries, whereas a perfectly circular watershed is indicated by a Cc value of 1. By influencing runoff concentration time and flow dynamics, the Cc directly affects soil erosion processes. Due to shorter flow routes, watersheds with low Cc (around 1) typically have fast peak discharges, which can result in concentrated erosion near the outlet, including gullying and channel scouring. On the other hand, runoff convergence is slowed down by high Cc values (elongated/irregular forms), which prolongs water flow down slopes and increases sheet and rill erosion. Furthermore, because of effective sediment transport, compact (low Cc) watersheds frequently show larger sediment yields during storms, whereas extended basins may see more sediment deposition along flow pathways (Nasir et al., 2023). Thus, the Compactness Coefficient is a critical indicator of erosion patterns, helping guide soil conservation strategies such as terracing (for elongated basins) or check dams (for compact basins) to mitigate erosion risks.

The C_c can be expressed mathematically by Equation 4 (Horton, 1945.

$$C_C = \frac{P}{2\sqrt{\pi A}} \cdots Equation. 4$$

Where A is the Area of the watershed in Km^2

and P is the watershed Paremeter in Km $$\pi$$ is the mathamatical constant (approximatly 3.14159)

 $Kalash \ watershed \ area = 511.72 \ km^2$ $Watershed \ Perimeter = 110.67 \ km$

$$Cc = \frac{110.67}{2\sqrt{3.14159 \times 511.72}}$$

$$Cc = \frac{110.67}{2\sqrt{1607.61}}$$

$$Cc = \frac{110.67}{2 \times 40.095}$$

$$Cc = \frac{110.67}{80.190}$$

$$Cc = 1.38$$

The computed Compactness Coefficient (C_c) of the KRW is 1.38, which is indicative of a moderately elongated and irregular shape, deviating significantly from a perfect circle (C_c = 1). This morphometric characteristic implies that the watershed has a longer perimeter relative to its area, leading to longer flow paths and slower concentration of runoff compared to a circular basin. As a result, peak discharges are less intense but more prolonged, increasing the duration of overland flow and promoting soil erosion across the watershed. The elongated shape also causes greater sediment deposition along channels due to reduced flow velocities, potentially leading to watershed aggradation. The higher C_c value suggests that soil erosion in the KRW is more spatially distributed rather than concentrated near the outlet, requiring erosion control measures.

4.1.8 Sediment Production Rate

The SPR refers to the quantity of sediment eroded and transported from a watershed over a specific period, typically measured in tons per hectare per year (t/ha/yr) or megagrams per square kilometre per year (Mg/km²/yr). SPR is a critical parameter in soil erosion studies, watershed management, and reservoir sedimentation assessments (Borrelli et al., 2022). It depends on factors such as watershed morphometry, specifically circulatory ratio, form factor, and compactness coefficient, climate, topography, land use, soil type, and anthropogenic activities (García-Ruiz et al., 2017).

4.2 Factors Influencing Sediment Production Rate

4.2.1 Climatic Factors

Rainfall Intensity: High-intensity rainfall increases soil erosion and runoff, overland flow, and accelerates sediment detachment (Panagos et al., 2022). In cold regions, melting snow contributes to sediment transport (Li et al., 2020).

4.2.2 Topographic Factors

Slope Gradient & Length and Morphometry: Steeper slopes enhance runoff velocity, increasing sediment yield (Singh & Jain 2024). Similarly, watershed Morphometry also affects the sediment production rate at a watershed. Compact watersheds (low Compactness Coefficient), high form factor, and high circulatory ratio produce higher sediment due to rapid runoff concentration (Horton, 1945).

4.2.3 Soil & Land Use Factors

Loamy and sandy gravelly soils erode faster than clayey soils (Wischmeier & Smith, 1978). Bare soils and improper farming increase soil erosion (Borrelli et al., 2022). Construction activities amplify sediment-laden runoff (Wolman, 1967).

4.2.4 Anthropogenic & Geological Factors

Accelerate sediment production via land disturbance due to mining and construction (Kondolf et al., 2018). Earthquakes and landslides trigger catastrophic sediment fluxes (Korup, 2012).

4.3 Sediment Production Rate of KRW

The watershed's shape affects the SPR because it dictates how rapidly runoff converges at the basin's outlet. Researchers have created empirical models based on geomorphological features to assess soil erosion and sediment output. To help with erosion prediction and control, Jose and Das (1982) and Reid and Dunne (1984) first developed the Sediment Production Rate (SPR) by correlating watershed topography with sediment dynamics. The morphometry-based sediment production rate (SPR) approach utilizes quantitative watershed characteristics to estimate soil erosion potential through geospatial analysis. This technique combines topography characteristics from digital elevation models (DEMs) with important MPs like Dd, Rb, and Cc. Studies reveal a substantial correlation between morphometric indices and measured sediment yields, particularly in mountainous regions where basin relief and slope steepness have a

direct impact on erosion processes (Rai et al., 2017). Because morphometric analysis only needs topographic data to provide accurate sediment yield estimates when calibrated with field measurements, the method is especially useful in areas with limited data (Horton, 1945). By identifying non-linear correlations between morphometric factors and sediment production rates, recent developments use machine learning to improve predictions (Arabameri et al., 2020). In emerging mountainous locations like the Himalayas, this approach provides an affordable substitute for intricate process-based models, particularly for preliminary watershed evaluations and the prioritization of erosion-prone sites for conservation planning.

The sediment production rate for the KRW was determined using eq. 5

$$Log SPR = 4919.80 + 48.64 log (100 + F_f)$$

 $-1337.77 \log(100 + R_c)$

$$-1165.65log (100 + C_c)...$$
 Equation. 5

Where Log SPR is the Sediment Production Rate, (ha

$$-m/100km^2/year$$
,

year,
$$F_f = \dot{F}orm\ Factor$$
, $R_c = Circulatory\ ratio$, $C_c = Compactness\ Coefficient$

Sediment Production Based on Form Factor

$$Log SPR = 4919.80 + 48.64 log(100 + F_f)$$

Constant	Form Factor	100+R _F	Log of 100+Rf	Constant	log*48.64	4919.8*log*48.64
4919.8	0.65	100.65	2.002813779	48.64	97.41686222	5017.216862

Sediment Production Based on Circulatory Ratio

$$R_c = 1337.77 \log(100 + R_c)$$

Constant	Circulatory Ratio (R _c)	100+R _c	Log(100+R _c)	1337.77*log (100+R _c)
1337.77	0.52	100.52	2.00225248	2678.5533

Sediment Production Based on Compactness Coefficient

 $Cc = 1165.65log (100 + C_c)$

Constant	Compactness Coefficient (C _c)	100+C _c	log (100 + C _c)	1165.65* log (100+C₀)
1165.65	1.38	101.38	2.005952287	2338.238283

Overall Sediment Production

$$Log SPR = 4919.80 + 48.64 log (100 + F_f)$$
$$-1337.77 log (100 + R_c) - 1165.65 log (100 + C_c)$$

Geospatial Modeling of Soil Erosion Dynamics in the Kalash River Watershed of District Chitral, Pakistan

Α	В	С	Sediment Production	
4919.8*log*48.64	1337.77*log	1165.65* log		
	(100+R _c)	(100+C _c)	(A-B-C)	
5017.216862	2678.5533	2338.238283	0.425279	

The sediment production rate of 0.43 hectare-meters per 100 square kilometres per year (ha-m/100 km²/year) in the KRW indicates the average amount of sediment eroded and transported out of the watershed annually. A rate of 0.43 ha-m/100 km²/year suggests moderate erosion, but the actual impact depends on soil type, slope, rainfall intensity, and land use of the study area. The sediment volume (0.43 ha-m) means 1 hectare-meter (ha-m) = 10,000 m³ (since 1 hectare = 10,000 m² and 1 m depth over that area = 10,000 m³). 0.43 ha-m = 4,300 m³ of sediment is produced per year. Area Normalization (per 100 km²), the rate is standardized per 100 square kilometers (km²) to allow comparison with other watersheds. The KRW is larger than 100 km², and the total sediment yield is scaled up proportionally to 0.43 ha-m/100 sq km/year.

4.4Stream Power Index (SPI) and Sediment Transport Index (STI)

The SPI and STI are the geomorphological and hydrological indices employed to calculate the fluvial erosion potential across a terrain. Stream power is a simple combination of stream flow, slope, and water pressure that is directly linked to sediment transportation (Abdelkrim et al., 2024). Hydrologists commonly use stream power because it can be potentially estimated remotely without requiring significant field observation. It considers both upstream contributing area (flow accumulation) and slope gradient to identify regions where water flow is expected to produce major erosion, sediment transport, or channel development. SPI assists in identifying zones with significant erosive potential (Zumara & Nasher, 2024). SPI is generally expressed mathematically as Equation 6:

Where:

Flow Accumulation = Number of cells draining into a given cell, 0.001 = Small constant added to avoid undefined values (log(0)), ln = Natural logarithm (scales values for better interpretation), Slope = Steepness of the terrain (in degrees or per cent).

The STI is expressed as equation 7, suggested by Moore and Burch (1986).

$$STI = (As/22.13)) ^m \times Sin(B/0.0896) ^n \dots Equation. 7$$

Where:

A = Watershed area (Flow accumulation grid), m = Contributing area exponent (set 0.4), n = Slope exponent (set 1.4), B = Slope in degrees.

Higher values of the SPI and STI correspond to steep slopes and the downstream portion of the watershed, both of which have a high rate of soil erosion (Singh et al., 2025). The lowest SPI values suggest slower sediment transport and correspond to watershed areas that are vegetated and have gentle slopes. The high SPI indicates concentrated water flow and steep slopes (high erosion risk). Very low (Negative or near-zero) SPI values indicate flat or low-flow zones with minimal erosion. Low to moderate SPI values suggest gentle slopes with moderate flow. The high SPI values are associated with steeper slopes with significant flow accumulation and a high risk of erosion. Figure. 5A, 5B, 5C, and 5D illustrate computed SPI values, Geology and Formation of the study area, STI, and Land Use Land Cover of the study area, respectively. Figure. 6A illustrates the computed SPI values and various slope classes for the KRW, and Figure. 6B illustrates the drainage density for the KRW.

Sediment transport index values in the KRW are higher along the 3rd and 4th order streams and lower parts of the watershed, indicating significant soil erosion and soil loss along the larger tributaries of the Kalash River, as shown in Figure 5C. The dense vegetation areas had the lowest STI values, which indicate slow sediment transport and sediment accumulation. The lower STI values correspond to the upstream areas of the KRW, which have considerable vegetation cover. The distribution of STI values correlates well with overall erosion assessments, as it shows sediment flow convergence and divergence from mountain tops to the lower parts, which are more susceptible to flooding and sedimentation. The study results correlate with the findings of Ahmad et al. (2019), Nadia et al. (2022), and Tilahun & Desta (2023).

Figure 7 shows the percentage area under various SPI classes. Table 4 presents the distribution of Stream Power Index (SPI) classes across a total area of 511.72 km², along with their respective percentages. The analysis reveals that most of the area is classified as no erosion, which is 502.91 km² (98.28%), indicating minimal to no erosion risk. A small portion, 3.47 km² (0.68%), falls under low erosion, while moderate erosion covers only 2.81 km² (0.55%). Areas with high erosion account for 1.63 km² (0.32%), and very high erosion is the least prevalent, covering just 0.90 km² (0.18%). The data highlights that erosion risk is relatively low across most of the region, with only a minor fraction experiencing moderate to very high erosion levels.

Over 98% of the watershed has low SPI values, indicating minimal to no erosion risk. This is likely due to stable land use (e.g., forests, grasslands) and resistant geology (e.g., hard rock formations) that prevent erosion. Figure 5A suggests that higher SPI values (indicating greater erosion potential) are found mostly along 3rd and 4th-order streams (mid-sized channels) in the lower part of the watershed. These areas coincide with intensive agricultural activity, suggesting that farming practices (e.g., ploughing, vegetation removal) may be increasing erosion risk by exposing soil to water flow. The upper and middle parts of the watershed are likely more stable due to natural land cover or less disturbance.

Table 4: Showing computed Stream Power Index and Area under each Class

Stream Power Index Classes (SPI)	Area in Km ²	%age of Total Area
	F02.01	00.20
No Erosion	502.91	98.28
Low Erosion	3.47	0.68
Moderate Erosion	2.81	0.55
High Erosion	1.63	0.32
Very High Erosion	0.90	0.18
	511.72	100.00

Source: DEM Analysis in ArcMap 10.8

Figure 5B illustrates the geology of the study area. The geology of the KRW plays a significant role in determining its resistance to soil erosion. The varying lithologies exhibit different responses to weathering and erosion, influencing landscape stability and sediment yield. Pre-Collision Intrusive rocks are likely comprised of granitic or gabbroic intrusions formed before the Himalayan orogeny. Generally high due to their massive, crystalline nature. However, jointed or fractured zones may be more susceptible to mechanical weathering and erosion. Form resistant ridges, contributing to steep slopes but limiting widespread soil loss unless deeply weathered. Karakoram Metamorphic Complex comprises high-grade metamorphic rocks (e.g., gneisses, schists) with varying mineralogy. These rocks have moderate resistance to soil erosion except where rocks are well-foliated and compact, but schistosity can lead to exfoliation and sheet erosion.

Reshun Marble is composed of metamorphosed carbonate rock (marble). Low to moderate resistance to soil erosion. Chitral Slate is fine-grained, low-grade metamorphic rock. Its resistance to soil erosion is low due to weak cleavage planes, making it prone to flaking, sliding, and gully erosion. Koghuzi Greenschist and Calcareous Phyllite are composed of low-grade metamorphic rocks (greenschist facies) with phyllitic foliation and

calcareous content. These rocks have moderate resistance to soil erosion. The watershed's erosion susceptibility is highly variable, with resistant intrusive and high-grade metamorphic rocks stabilizing large areas, while slate, phyllite, and marble contribute disproportionately to the sediment load.

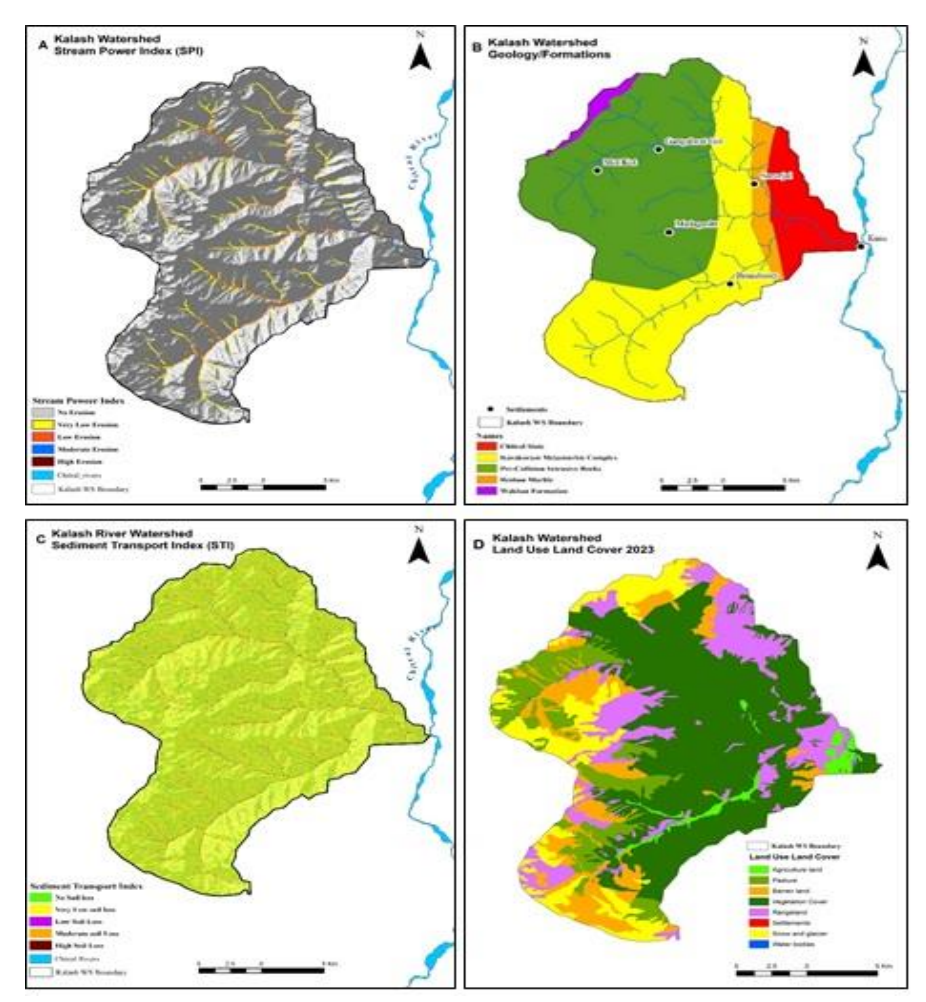


Figure 5. (5A) illustrates the computed SPI values for the Kalash River watershed, (5B) Geology and Formation of the study area, (5C) Sediment Transport Index, and (5D) Showing Land Use Land Cover of the study area.

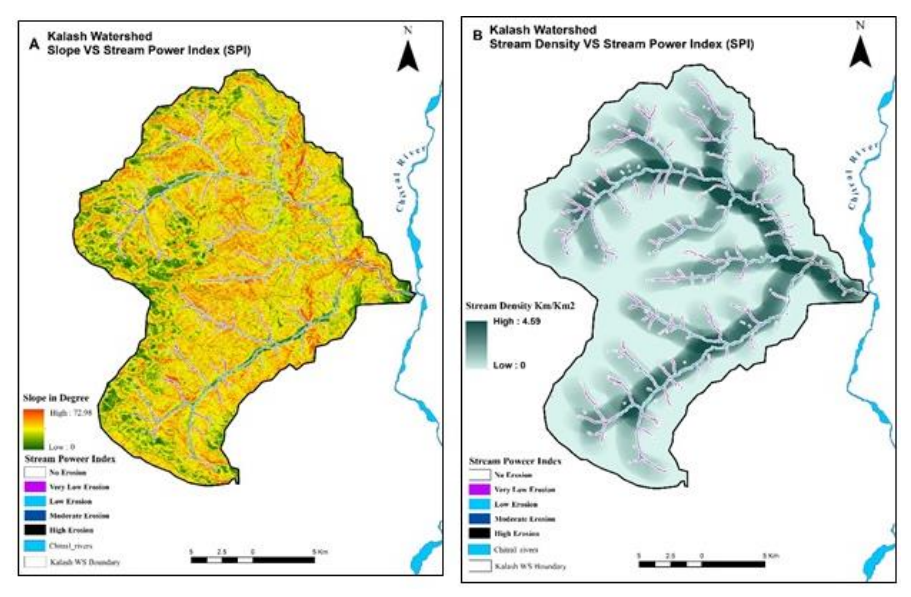


Figure 6. (6A) illustrates the slope VS computed SPI values for the KRW, (6B) shows the drainage density of the study area.

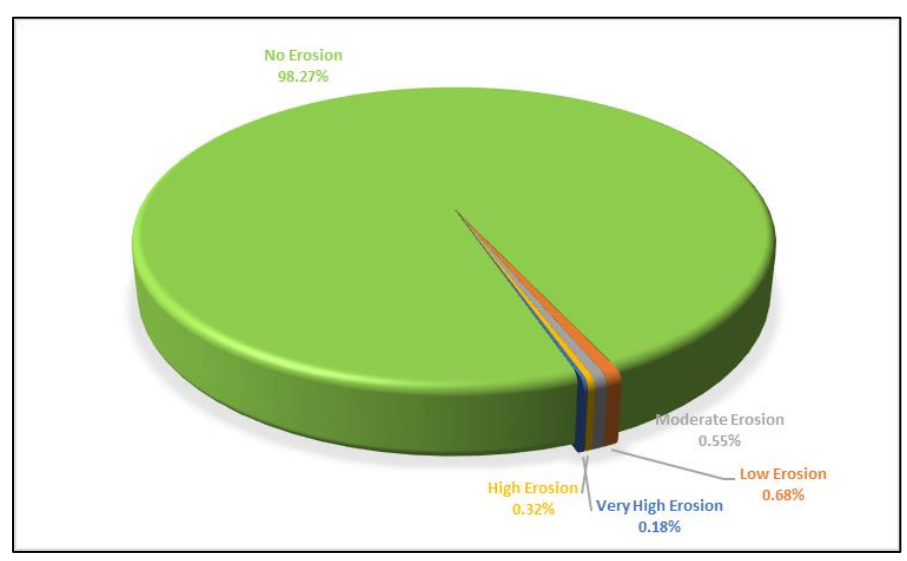


Figure 7. Showing computed Stream Power Index and Area under each Class

5. CONCLUSION

The morphometric characteristics of the KRW give us a clear picture of how sediment moves through the watershed, where erosion is likely to happen, and how the water behaves overall. The drainage network is well developed and dendritic, with a fourth-order stream system fed by many first-order tributaries, basically a very branched, tree-like pattern. When

we look at parameters like stream order, bifurcation ratio, circulatory ratio (0.52), form factor (0.65), and compactness coefficient (1.38), the basin comes out semi-circular to slightly elongated. That shape affects both runoff concentration and sediment transport. Overall, the combination of gentle slopes, land-use patterns, and the underlying geology keeps erosion mild, with an average sediment yield of just 0.43 ha-m/100 km²/year. The Stream Power Index (SPI) shows that more than 98 % of the area has very low erosion risk. The only spots with somewhat higher potential are the mid-sized streams running through agricultural land. Geologically, the watershed sits on pre-Collision intrusive rocks and parts of the Karakoram Metamorphic Complex. The more resistant rock units provide good stability, whereas fractured or foliated zones are the main sources of the limited sediment we do see. All these points highlight the importance of putting in place proper integrated watershed management, especially in the few vulnerable areas, so we can minimize soil loss and keep the hydrological system sustainable in the long run.

REFERENCES

Abdelkrim, Z., Faid, B., & Eslamian, S. (2024). Sediment Transport Index and Stream Power Index Using GIS: A Case Study in the Bou Saâda Wadi—Sub-basin, Algeria. In *Handbook of Climate Change Impacts on River Basin Management* (pp. 164-173). CRC Press.

Ahmad, I., Dar, M. A., Teka, A. H., Gebre, T., Gadissa, E., & Tolosa, A. T. (2019). Application of hydrological indices for erosion hazard mapping using Spatial Analyst tool. *Environmental monitoring and assessment*, 191(8), 482.

Akhtar, Z., Nasir, M. J., Ali, Z., Zahid, S. M. H., Iqbal, S., & Khan, Z. (2024). Sediment Yield Estimation Using Gis-Based Sediment Production Rate (Spr) Approach: A Study of Kunhar River Basin, Pakistan. *Migration Letters*, *21*(S11), 111-134.

Arabameri, A., Saha, S., Roy, J., Chen, W., Blaschke, T., & Tien Bui, D. (2020). Landslide susceptibility evaluation and management using different machine learning methods in the Gallicash River Watershed, Iran. *Remote Sensing*, *12*(3), 475.

Ashraf, A., & Ahmad, I. (2024). Evaluation of soil loss severity and ecological restoration approach for sustainable agriculture in the Hindu Kush, Karakoram and Himalaya region. *Journal of Mountain Science*, *21*(5), 1509-1521.

Aslam, B., Maqsoom, A., Alaloul, W. S., Musarat, M. A., Jabbar, T., & Zafar, A. (2021). Soil erosion susceptibility mapping using a GIS-based multi-

criteria decision approach: Case of district Chitral, Pakistan. *Ain Shams Engineering Journal*, 12(2), 1637-1649.

Boota, M. W., Soomro, S. E. H., Xia, H., Qin, Y., Azeem, S. S., Yan, C., ... & Boota, M. A. (2024). Estimation of soil loss and sediment yield by using the modified RUSLE model in the Indus River basin, including the quantification of error and uncertainty in remote-sensing images. *Marine and Freshwater Research*, 75(17), MF24082.

Borrelli, P., Ballabio, C., Yang, J. E., Robinson, D. A., & Panagos, P. (2022). GloSEM: High-resolution global estimates of present and future soil displacement in croplands by water erosion. *Scientific Data*, *9*(1), 406.

Cárceles Rodríguez, B., Durán-Zuazo, V. H., Soriano Rodríguez, M., García-Tejero, I. F., Gálvez Ruiz, B., & Cuadros Tavira, S. (2022). Conservation agriculture as a sustainable system for soil health: A review. *Soil Systems*, *6*(4), 87.

Eloudi, H., Hssaisoune, M., Reddad, H., Namous, M., Ismaili, M., Krimissa, S., ... & Bouchaou, L. (2023). Robustness of optimized decision tree-based machine learning models to map gully erosion vulnerability. *Soil Systems*, 7(2), 50.

Farhan, Y., & Anaba, O. (2016). A remote sensing and GIS approach for prioritization of Wadi Shueib mini-watersheds (Central Jordan) based on morphometric and soil erosion susceptibility analysis. *Journal of Geographic Information System*, 8(01), 1.

García-Ruiz, J. M., Beguería, S., Lana-Renault, N., Nadal-Romero, E., & Cerdà, A. (2017). Ongoing and emerging questions in water erosion studies. *Land Degradation & Development*, 28(1), 5-21.

Gilani, H., Ahmad, A., Younes, I., & Abbas, S. (2022). Impact assessment of land cover and land use changes on soil erosion changes (2005–2015) in Pakistan. *Land Degradation & Development*, 33(1), 204-217.

Grecu, F., Zaharia, L., Ioana-Toroimac, G., & Armaş, I. (2017). Floods and flash-floods related to river channel dynamics. *Landform dynamics and evolution in Romania*, 821-844.

Hasnaoui, Y., Tachi, S. E., Bouguerra, H., & Yaseen, Z. M. (2025). Transfer learning-based deep learning models for flood and erosion detection in coastal area of Algeria. *Earth Science Informatics*, *18*(2), 380.

Hitouri, S., Varasano, A., Mohajane, M., Ijlil, S., Essahlaoui, N., Ali, S. A., ... & Teodoro, A. C. (2022). Hybrid machine learning approach for gully erosion mapping susceptibility at a watershed scale. *ISPRS International Journal of Geo-Information*, 11(7), 401.

Horton, R. E. (1945). Erosional development of streams and their drainage basins; hydrophysical approach to quantitative morphology. *Geological society of America bulletin*, *56*(3), 275-370.

Jothimani, M., Abebe, A., & Dawit, Z. (2020). Mapping of soil erosion-prone sub-watersheds through drainage morphometric analysis and weighted sum approach: a case study of the Kulfo River basin, Rift valley, Arba Minch, Southern Ethiopia. *Modeling Earth Systems and Environment*, 6, 2377-2389.

Jose, C. S., & Das, D. C. (1982, November). Geomorphic prediction models for sediment production rate and intensive priorities of watersheds in Mayurakshi catchment. In *Proc. Int. Symp. on Hydrological Aspects of Mountainous Watershed, School of Hydrology, University of Roorkee* (Vol. 1, pp. 15-23).

Kousar, S., & Shirazi, S. A. (2023). Spatio-temporal variations of land-use land-cover in response to RUSLE Model in Swat basin using remote sensing and GIS techniques. *Sarhad Journal of Agriculture*, 39(3), 722-737.

Kondolf, G. M., Schmitt, R. J., Carling, P., Darby, S., Arias, M., Bizzi, S., ... & Wild, T. (2018). Changing sediment budget of the Mekong: Cumulative threats and management strategies for a large river basin. *Science of the total environment*, *625*, 114-134.

Korup, O. (2012). Landslides in the Earth system. *Landslides: Types, Mechanisms and Modeling. Cambridge University Press, Cambridge*, 10-23.

Kumar, S., David Raj, A., Kalambukattu, J.G., Chatterjee, U. (2022). Climate Change Impact on Land Degradation and Soil Erosion in Hilly and Mountainous Landscape: Sustainability Issues and Adaptation Strategies. *Ecological Footprints of Climate Change. Springer Climate. Springer, Cham.* https://doi.org/10.1007/978-3-031-15501-7_5

Li, D., Li, Z., Zhou, Y., & Lu, X. (2020). Substantial increases in the water and sediment fluxes in the headwater region of the Tibetan Plateau in response to global warming. *Geophysical Research Letters*, 47(11), e2020GL087745.

Maqsoom, A., Aslam, B., Hassan, U., Kazmi, Z. A., Sodangi, M., Tufail, R. F., & Farooq, D. (2020). Geospatial assessment of soil erosion intensity and sediment yield using the revised universal soil loss equation (RUSLE) model. *ISPRS International Journal of Geo-Information*, *9*(6), 356.

Mehwish, M., Nasir, M. J., Raziq, A., Al-Quraishi, A. M. F., & Ghaib, F. A. (2024). Soil erosion vulnerability and soil loss estimation for Siran River watershed, Pakistan: an integrated GIS and remote sensing approach. *Environmental Monitoring and Assessment*, 196(1), 104.

- Merritt, W. S., Letcher, R. A., & Jakeman, A. J. (2003). A review of erosion and sediment transport models. *Environmental modelling & software*, 18(8-9), 761-799.
- Miller, V. C. (1953). A quantitative geomorphic study of drainage basin characteristics in the Clinch Mountain area, Virginia and Tennessee (Vol. 3). New York: Columbia University.
- Morgan, R. P. C., Quinton, J. N., Smith, R. E., Govers, G., Poesen, J. W. A., Auerswald, K., ... & Styczen, M. E. (1998). The European Soil Erosion Model (EUROSEM): a dynamic approach for predicting sediment transport from fields and small catchments. *Earth Surface Processes and Landforms: The Journal of the British Geomorphological Group*, 23(6), 527-544.
- Musa, I. O., Samuel, J. O., Adams, M., Abdulsalam, M., Nathaniel, V., Maude, A. M., ... & Tiamiyu, A. G. T. (2024). Soil erosion, mineral depletion and regeneration. In *Prospects for soil regeneration and its impact on environmental protection* (pp. 159-172). Cham: Springer Nature Switzerland.
- Nadia, E., Hasan, O., Said, H., & Mohamed, A. (2022). Sediment Transport Index (STI) Modeling using the GIS at Small Agricultural Catchment. *International Journal of Innovative Research in Sciences and Engineering Studies (IJIRSES)*, 2(11).
- Nasir, M. J., Khan, A. S., Alam, S., & Mehmood, K. (2025). Morphometric Analysis of Beshigram Watershed in Swat Valley, Eastern Hindukush, Using GIS and Remote Sensing Techniques. *The Sciencetech*, 151-171.
- Nasir, M. J., Ahmad, W., Jun, C., Iqbal, J., & Bateni, S. M. (2023). Soil erosion susceptibility assessment of Swat River sub-watersheds using the morphometry-based compound factor approach and GIS. *Environmental Earth Sciences*, 82(12), 315.
- Naqvi, S. A. A., Tariq, A., Shahzad, M., Khalid, S., Tariq, Z., Salma, U., ... & Soufan, W. (2024). Predicting soil erosion risk using the revised universal soil loss equation (RUSLE) model and geo-spatial methods. *Hydrological Processes*, *38*(8), e15248.
- Nigussie, A. B., Ayeled, G. T., Endalew, A., Miheretu, B. A., Amognehegn, A. E., Adamu, A. Y., & Karuppannan, S. (2025). Integrating Google Earth Engine and GIS for RUSLE-based soil erosion and sediment yield assessment in Borkena Watershed, Ethiopia. *Journal of Sedimentary Environments*, 10(1), 197-219.
- Panagos, P., Borrelli, P., Matthews, F., Liakos, L., Bezak, N., Diodato, N., & Ballabio, C. (2022). Global rainfall erosivity projections for 2050 and

- 2070. *Journal of Hydrology*, *610*, 127865.Panda, S. (2022). *Soil and Water Conservation for Sustainable Food Production*. Springer Nature.
- Pimentel, D., & Burgess, M. (2013). Soil erosion threatens food production. *Agriculture*, *3*(3), 443-463.
- Rai, P. K., Mishra, V. N., & Mohan, K. (2017). A study of morphometric evaluation of the Son basin, India using geospatial approach. *Remote Sensing Applications: Society and Environment*, 7, 9-20.
- Rashmi, I., Karthika, K. S., Roy, T., Shinoji, K. C., Kumawat, A., Kala, S., & Pal, R. (2022). Soil Erosion and sediments: a source of contamination and impact on agriculture productivity. In *Agrochemicals in Soil and Environment: Impacts and Remediation* (pp. 313-345). Singapore: Springer Nature Singapore
- Reid, L. M., & Dunne, T. (1984). Sediment production from forest road surfaces. *Water Resources Research*, 20(11), 1753-1761.
- Rojas, R. V., Achouri, M., Maroulis, J., & Caon, L. (2016). Healthy soils: a prerequisite for sustainable food security. *Environmental Earth Sciences*, 75, 1-10.
- Sanz, M. J., de Vente, J., Chotte, J. L., Bernoux, M., Kust, G., Ruiz, I., ... & Akhtar-Schuster, M. (2017). Sustainable land management contribution to successful land-based climate change adaptation and mitigation: A report of the science-policy interface. In *Bonn, Germany: United Nations Convention to Combat Desertification (UNCCD)*.
- Singh, O., & Singh, J. (2018). Soil erosion susceptibility assessment of the lower Himachal Himalayan Watershed. *Journal of the Geological Society of India*, *92*, 157-165.
- Singh, P. K., & Jain, S. K. (2024). Soil Erosion and Sediment Yield Modeling. In *Handbook of Climate Change Impacts on River Basin Management* (pp. 19-33). CRC Press.
- Singh, S., Swarnkar, S., & Sinha, R. (2025). Integrating sediment connectivity and stream power index with RUSLE for modelling soil erosion dynamics in a large Himalayan basin under modern and future climate scenarios. *Earth Surface Processes and Landforms*, *50*(3), e70032.
- Shekar, P. R., & Mathew, A. (2024). Morphometric analysis of watersheds: A comprehensive review of data sources, quality, and geospatial techniques. *Watershed Ecology and the Environment*, 6, 13-25.
- Siebielec, G., Suszek-topatka, B., & Maring, L. (2016). The impact of soil degradation on human health. *Science*, *7*, 374-392.

Strahler, A. N. (1964). Part II. Quantitative geomorphology of drainage basins and channel networks. *Handbook of Applied Hydrology: McGraw-Hill, New York*, 4-39.

Tedoldi, D., Chebbo, G., Pierlot, D., Kovacs, Y., & Gromaire, M. C. (2016). Impact of runoff infiltration on contaminant accumulation and transport in the soil/filter media of Sustainable Urban Drainage Systems: A literature review. *Science of the Total Environment*, *569*, 904-926.

Tilahun, A., & Desta, H. (2023). Soil erosion modeling and sediment transport index analysis using USLE and GIS techniques in Ada'a watershed, Awash River Basin, Ethiopia. *Geoscience Letters*, 10(1), 57.

Waikar, M. L., & Nilawar, A. P. (2014). Morphometric analysis of a drainage basin using geographical information system: a case study. *Int J Multidiscip Curr Res*, 2(2014), 179-184.

Wischmeier, W. H., & Smith, D. D. (1978). *Predicting rainfall erosion losses:* a guide to conservation planning (No. 537). Department of Agriculture, Science and Education Administration

Wolman, M. G., & Schick, A. P. (1967). Effects of construction on fluvial sediment, urban and suburban areas of Maryland. *Water Resources Research*, 3(2), 451-464.

Zineddine, F. E. R. K. H. I. (2025). *Predictive Modeling of Soil Erosion Using GIS and Artificial Intelligence. Tafna watershed case* (Doctoral dissertation, univercity centre of abdelhafid boussouf mila).

Zumara, R., & Nasher, N. R. (2024). Soil erodibility mapping of hilly watershed using analytical hierarchy process and geographical information system: A case of Chittagong hill tract, Bangladesh. *Heliyon*, *10*(5).